Adlayer Structure of and Electrochemical O_2 Reduction on Cobalt Porphine-Modified and Cobalt Octaethylporphyrin-Modified Au(111) in $HClO_4$

Soichiro Yoshimoto,[†] Junji Inukai,[†,‡] Akinori Tada,[†] Toru Abe,[†] Tatsuki Morimoto,[§] Atsuhiro Osuka,[§] Hiroyuki Furuta,[||] and Kingo Itaya*[,†,⊥]

Department of Applied Chemistry, Graduate School of Engineering, Tohoku University, Aoba-yama 04, Sendai 980-8579, Japan, New Industry Creation Hatchery Center, Tohoku University, Aoba-yama 10, Sendai 980-8579, Japan, CREST-JST, Kawaguchi Center Building, 4-1-8 Honcho, Kawaguchi, Saitama 332-0012, Japan, Department of Chemistry, Graduate School of Science, Kyoto University, Kyoto 606-8502, Japan, and Department of Chemistry and Biochemistry, Graduate School of Engineering, Kyushu University, Fukuoka 812-8581, Japan

Received: September 4, 2003; In Final Form: October 31, 2003

Adlayers of cobalt(II) porphine (CoP) and [2,3,7,8,12,13,17,18-octaethyl-21*H*,23-*H*-porphine]cobalt(II) (CoOEP) were formed on Au(111) by immersing the substrate in a benzene solution containing either CoP or CoOEP molecules and investigated in 0.1 M $HClO_4$ by using in situ scanning tunneling microscopy. Highly ordered arrays of CoP were observed on the Au(111)-(1×1) surface under controlled potential conditions. The adlayer of CoOEP molecules was also highly ordered, whereas the Au(111) substrate was found to become reconstructed upon adsorption of CoOEP. Both CoP and CoOEP molecules were closely packed on Au(111). On the adlayers of CoP and CoOEP, the electrochemical reduction of O_2 was examined in 0.1 M $HClO_4$ saturated with O_2. The adlayers of both CoP and CoOEP on Au(111) enhanced the reduction of O_2.

Introduction

Formation and characterization of ordered adlayers of porphyrin molecules at electrolyte-electrode interfaces are important from the fundamental and technological points of view. Porphyrins are of great interest in such diversified fields as biology,[1] photosynthesis,[1] electrocatalysis,[2,3] and molecular devices.[4] In electrochemistry, thin films of metalloporphyrins and their derivatives have been intensively studied for the interest in electrocatalytic reactions, such as the reduction of O_2, mainly at graphite electrodes.[2,3,5−10] For example, Anson and co-workers reported a two-step 4-electron reduction of O_2 on graphite electrodes with adlayers of cobalt(II) porphine (CoP),[8] [2,3,7,8,-12,13,17,18-octaethyl-21*H*,23*H*-porphine]cobalt(II) (CoOEP),[9] and other cobalt porphyrins.[9,10]

Adlayer structures of porphyrins were studied in the past mostly in ultrahigh vacuum (UHV) using scanning tunneling microscopy (STM) on various metal surfaces.[11−16] Gimzewski and co-workers investigated [5,10,15,20-tetrakis(3,5-di-*tert*-butylphenyl)porphine]copper(II) (CuTBPP) on Cu(100), Au-(110), and Ag(110) in UHV.[11] They found that the packing arrangement of CuTBPP depends on the metal substrate used.[11] Yokoyama et al. found that the CN-substituted TBPP molecules adsorbed on Au(111) formed supermolecular assemblies such as trimers, tetramers, and extended wire-like structures.[12,13] Recently, the adlayer of NiOEP prepared by sublimation in UHV was also investigated on Au(111) by Hipps' group, who found that the NiOEP molecules were arranged alternately with a rotation angle of 15°.[14]

STM has also been used to understand the structure of adlayers of porphyrin molecules in solution.[17−24] We previously reported that highly ordered arrays of water-soluble 5,10,15,-20-tetrakis(*N*-methylpyridinium-4-yl)-21*H*,23*H*-porphine (H_2-TMPyP) molecules were formed on the iodine-modified (I-) Au(111),[17−19] I−Ag(111),[20] I−Pt(100),[21] and sulfur-modified Au(111) electrodes.[22] In addition to symmetry and structure of the H_2TMPyP array, the STM image provided with a great deal of information concerning the internal molecular structure. Tao et al. also investigated the adlayers of three water-soluble molecules, iron(III) protoporphyrin(IX), zinc(II) protoporphyrin-(IX), and protoporphyrin(IX), on the graphite basal plane in aqueous solutions with both STM[23,24] and atomic force microscopy.[23] Similar adlayer structures were formed for the three molecules, although the internal structures obtained by in situ STM were significantly different.[23] Very recently, we succeeded in forming highly ordered molecular arrays of water-insoluble [tetraphenyl-21*H*,23*H*-porphine]cobalt(II) and -copper(II) (CoTPP and CuTPP),[25] spontaneously on Au(111) surfaces by immersing Au(111) in benzene solutions containing those molecules. The adlayers of CoTPP and CuTPP thus formed were observed in $HClO_4$ solutions, and the structures were found to be identical to those obtained in UHV reported previously by Hipps and co-workers.[15,16]

Porphine is the simplest porphyrin molecule, whose framework is the basis of all porphyrins as well as all phthalocyanines. Although various porphyrin derivatives have been investigated on surfaces, the monolayer structure of simple porphine molecules has not been investigated so far. In the present paper, we report the adlayer structures of CoP and its simple derivative, CoOEP (see Chart 1), on Au(111) in $HClO_4$ observed by using in situ STM. We also found that the electrochemical reduction of O_2 on Au(111) in $HClO_4$ is enhanced by CoP and CoOEP adlayers.

* To whom correspondence should be addressed. E-mail: itaya@atom.che.tohoku.ac.jp. Phone/Fax: +81-22-214-5380.
[†] Graduate School of Engineering, Tohoku University.
[‡] New Industry Creation Hatchery Center, Tohoku University.
[§] Kyoto University.
[||] Kyushu University.
[⊥] CREST-JST.

10.1021/jp0366421 CCC: $27.50
Published on Web 01/16/2004

CHART 1: Chemical Formulas of CoP and CoOEP Molecules

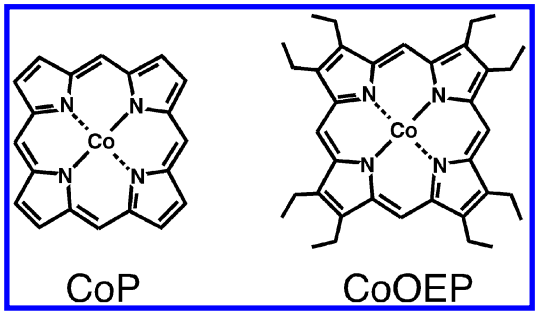

Experimental Section

CoP was synthesized by the procedure described in previous papers.[26−28] CoOEP was purchased from Aldrich and used without further purification. Benzene was obtained from Kanto Chemical Co. (Spectroscopy Grade). The electrolyte solution was prepared with $HClO_4$ (Cica-Merck) and ultrapure water (Milli-Q SP-TOC; ≥18.2 MΩ cm).

Au(111) single-crystal electrodes were prepared by the Clavilier method.[29] The aligned gold single-crystal bead was cut and successively polished with finer grades of alumina paste, and the electrode was then annealed at ca. 950 °C for at least 12 h in an electric furnace to remove mechanical damages. The electrode was finally annealed in a hydrogen flame and quenched into ultrapure water saturated with hydrogen to obtain Au(111)-(1×1).[25,30] Then, CoP and CoOEP adlayers were formed by immersing the Au(111) electrode into a 10 μM benzene solution containing either CoP or CoOEP for 50−60 s, in the same manner as that which we used previously for preparing the adlayers of coronene,[31,32] fullerene monomer C_{60} and fullerene dimer C_{120},[33] CoTPP,[25] and CoPc.[34] The CoP- or CoOEP-modified Au(111) electrode was then rinsed with ultrapure water, and it was transferred into an electrochemical cell for both voltammetric and STM measurements to prevent contamination.

Cyclic voltammetry was carried out under N_2 or O_2 at 20 °C with the hanging meniscus method in a three-compartment electrochemical cell using a potentiostat (HOKUTO HAB-151, Tokyo). The catalytic activity of the CoP- and CoOEP-modified Au(111) electrodes for the reduction of O_2 was examined in 0.1 M $HClO_4$ saturated with O_2 using the hanging meniscus rotating disk method[35] with a Model 636 ring-disk system (EG&G). Electrochemical STM measurements were performed by using a Nanoscope E (Digital Instruments, Santa Barbara, CA) with tungsten tips etched in 1 M KOH. To minimize residual faradic current, the tips were coated with nail polish. STM images were taken in the constant-current mode. All potentials are referred to a reversible hydrogen electrode (RHE) in 0.1 M $HClO_4$.

Results and Discussion

Voltammetry. Figure 1a shows cyclic voltammograms (CVs) recorded on a clean Au(111) electrode in 0.1 M $HClO_4$ under N_2 at the scan rate of 50 mV s^{-1}. Identical CVs were continuously obtained after potential cycles. In the double-layer potential region (dashed line in Figure 1a), two anodic peaks at 0.7 and 1.0 V and two cathodic peaks at 0.6 and 0.9 V were obtained.[36] In the anodic scan in a wider potential region (solid line in Figure 1a), oxidative current started at 1.19 V, and two oxidative peaks appeared at 1.35 and 1.60 V. In the cathodic scan, a sharp reduction peak was observed at 1.15 V with a shoulder peak at 1.1 V. These CV features were identical to those reported for a single-crystal Au(111) surface.[30,37] Figure 1b shows the CVs obtained with a CoP-modified Au(111). The open circuit potential (OCP) of the CoP-adsorbed Au(111) electrode was around 0.85 V, and the potential scan was started in the negative direction from the OCP. The decreased double-layer charging current shown by the dashed line in Figure 1b indicates that the Au(111) surface is covered with CoP molecules in this potential range. A reduction peak was seen at 0.31 V. Murray's group investigated a self-assembled monolayer of a CoTPP derivative, 5,10,15,20-tetrakis(*o*-(2-mercaptoethoxy)phenyl)porphyrin (Co(*o*-TMEPP)), on evaporated Au films.[38] The CV profile obtained in their study was similar to that in Figure 1b, and they attributed the peak to the reduction of Co(III) to Co(II).[38] The reduction peaks of Co(III) to Co(II) were also obtained at the CoTPP- and CoPc-modified Au(111) electrodes, as described in our previous papers.[25,34] Therefore, we also attribute the peak at 0.31 V in Figure 1b to the reduction of Co(III) to Co(II). The charge consumed at the peak was ca. 10 μC cm^{-2}, which is equivalent to a monolayer of CoP on Au(111). After the scanning between 0 and 0.9 V, the potential was scanned negatively first to −0.1 V and then positively up to 1.7 V. As shown by the solid line in Figure 1b, the anodic current commenced at 1.15 V, a potential more cathodic than

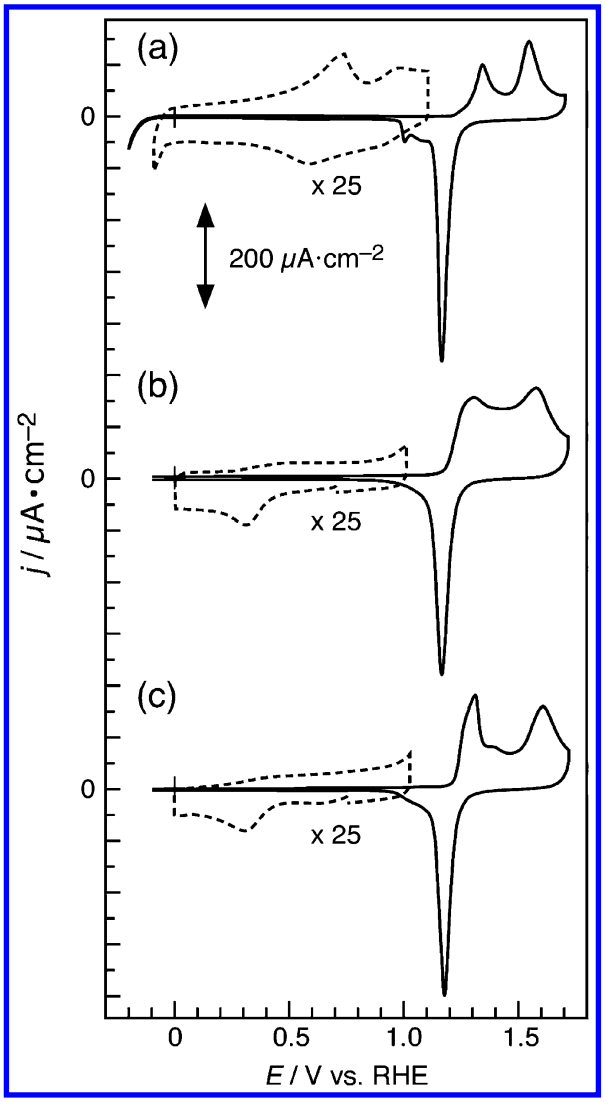

Figure 1. Cyclic voltammograms of bare (a), CoP-modified (b), and CoOEP-modified (c) Au(111) electrodes in 0.1 M $HClO_4$ under a N_2 atmosphere. The potential scan rate was 50 mV s^{-1}.

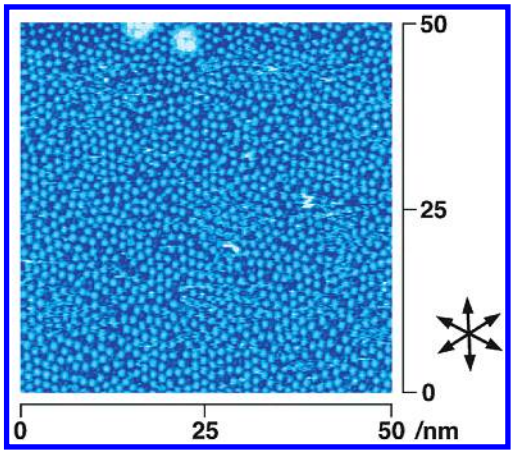

Figure 2. Large-scale (50 × 50 nm^2) STM image of the CoP adlayer on Au(111) surface in 0.1 M $HClO_4$ acquired at 0.85 V. The potential of the tip and tunneling current were 0.35 V and 1.0 nA, respectively.

that seen in Figure 1a, and the increase in current was steeper than that observed at the bare Au(111). Two broad oxidative peaks are seen at 1.3 and 1.6 V, and the sum of the charge densities of these peaks, 1300 μC cm^{-2}, is twice as large as that calculated for the two anodic peaks in Figure 1a, 680 μC cm^{-2}. It can thus be considered that the CoP molecules on the surface are oxidized simultaneously with the Au substrate at the potentials for the two anodic peaks. On the other hand, the charge density of the cathodic peak observed at 1.17 V in Figure 1b is the same as that seen in Figure 1a, indicating that the oxidative species related to CoP on the surface was not involved in this cathodic peak. As the scanning was repeated between −0.1 and +1.7 V, the CV profiles seen in Figure 1b became increasingly similar to those in Figure 1a; CoP was continuously oxidized and desorbed from the surface. Figure 1c shows the CV obtained on a CoOEP-adsorbed Au(111) electrode. The OCP of the CoOEP-modified Au(111) electrode was 0.85 V. The profile of the CV between 0 and 0.9 V (dashed line) is similar to that observed in Figure 1b with the reduction of Co(III) at 0.31 V. In the anodic scan up to 1.7 V (solid line), the steep increase in anodic current was observed at 1.17 V. Two oxidation peaks different from those in Figure 1a are seen at 1.2 and 1.6 V. In the cathodic scan, a reduction peak was observed at 1.19 V. The continuous scanning between −0.1 and +1.7 V also oxidized and desorbed CoOEP molecules from the surface as in the case of CoP discussed above.

In Situ STM. *(1) CoP Adlayer.* Figure 2 shows a typical STM image of a CoP adlayer on Au(111)-(1×1) acquired at the OCP (0.85 V) in 0.1 M $HClO_4$. In the image of a relatively large area of 50 × 50 nm^2, individual molecules can be recognized on atomically flat terraces. Although each CoP molecule can be discriminated, ordered domains are hardly seen (Figure 2). When the potential was kept at 0.8 V, a slightly negative potential than the OCP, some ordered domains began to appear gradually on the terrace, as shown by arrows in Figure 3a. Furthermore, when the potential was stepped from 0.8 to 0.75 V, highly ordered domains of CoP were formed. This ordering of porphyrins at negative potentials was also reported by Borguet and co-workers, due to the change in surface interactions.[39] Briefly, domains were composed of two regions marked I and II in Figure 3b. In region I, a densely packed phase is seen on the terrace, where CoP molecules are hexagonally arranged. The domain size was typically about 20 × 20 nm^2. In region II, CoP molecules are adsorbed in a disordered, random fashion, and the coverage is low.

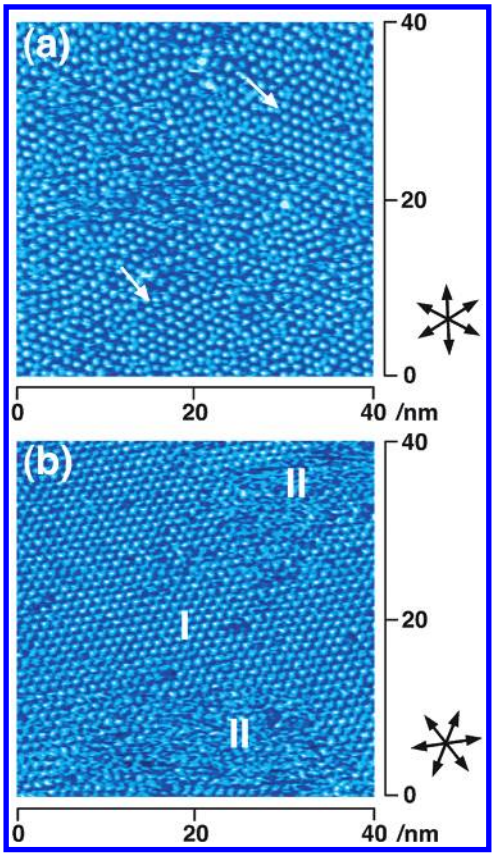

Figure 3. Large-scale (40 × 40 nm^2) STM images of the CoP adlayer on Au(111) surface in 0.1 M $HClO_4$ acquired at 0.8 V (a) and 0.75 V (b). The potential of the tip was 0.25 V, and tunneling currents were 10 nA (a) and 2.0 nA (b). The set of three arrows indicates the close-packed directions of Au(111) substrate.

To clarify structural details of the CoP adlayer in region I, a high-resolution STM image was recorded at 0.75 V. Figure 4a shows a typical high-resolution STM image acquired in an area of 9 × 9 nm^2, revealing clear internal molecular structures and molecular orientations in the ordered layers. An individual CoP molecule can be recognized as a square configuration with a bright spot at the center. At a cathodic potential of 0.1 V, identical STM images as shown in Figure 4a were also obtained. It has been reported by Hipps' group and our group that the center of each Co(II)−porphyrin molecule appears brightest in the STM image both in UHV[15,16] and in solution,[25] because of the tunneling being mediated by a half filled d_{z^2} orbital between the Au electrode and the tip. However, at the potential of 0.75 V, the center Co ion is in the state of Co(III) due to the electrochemical oxidation (Figure 1b); i.e., the d_{z^2} orbital should be empty. Another mechanism must be taken into account to explain the tunneling at the center position of Co(III) porphine in this oxidation state. It is generally known that Co(III) porphyrin is unstable and that it needs axial ligands, such as O_2, to be stabilized.[40] Because our STM measurements were carried out under atmospheric conditions, it is possible that O_2 molecules dissolved in solution were eventually attached to Co(III) ions to stabilize $Co^{III}P$. According to previous literature, stronger σ-donating axial ligands lead to smaller Co hyperfine couplings, promoting the localization of the π-electrons on the oxygen.[40] This π orbital might act as a new tunneling pathway, which could increase the tunneling current at the central position of $Co^{III}P$. A comparison between this image and that of atomic step lines reveals that the molecular rows in Figure 4a are aligned in the lattice directions of the Au(111) substrate. Molecular rows in Figure 4a cross each other at an angle of

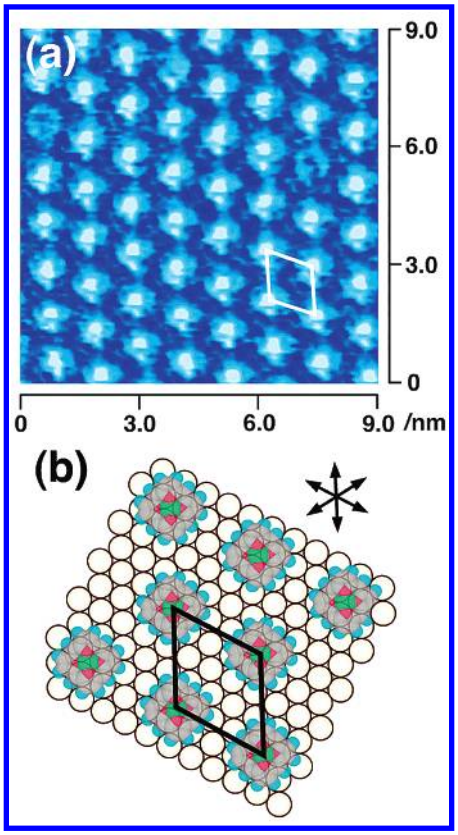

Figure 4. High-resolution (9 × 9 nm^2) STM image and structural model of close-packed CoP array in the CoP adlayer on Au(111) in 0.1 M $HClO_4$ acquired at 0.75 V. The potential of the tip and tunneling current were 0.35 V and 9.8 nA, respectively.

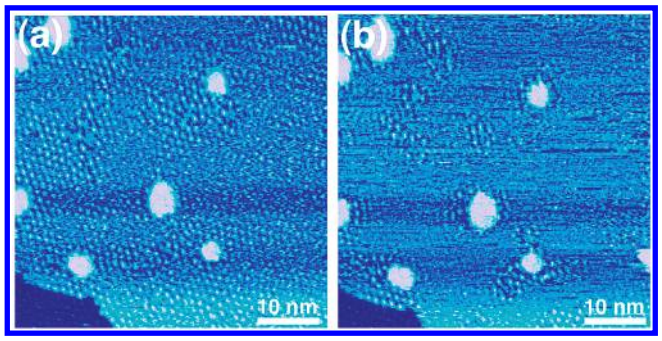

Figure 5. Large-scale (50 × 50 nm^2) STM images of the initial desorption process of CoP adlayer on Au(111) surface in 0.1 M $HClO_4$ acquired at 0 V. The potential of the tip was 0.45 V, and tunneling currents were 1.5 nA (a) and 1.25 nA (b).

60°. The intermolecular distance was found to be 1.18 ± 0.05 nm, that is, 4 times the atomic distance on Au(111)-(1×1) (1.156 nm). Therefore, the ordered adlayer structure obtained at 0.75 V was assigned to (4×4). The unit cell is superimposed in Figure 4a. Each unit cell includes one CoP molecule, which leads to a surface concentration of 1.44 × 10^{-10} mol cm^{-2}. A structural model for the CoP lattice is proposed in Figure 4b. Although the exact relationship between the CoP array and the underlying Au(111) lattice could not be determined in the present study, we placed the center of each CoP molecule at the 3-fold hollow site in this model. The closely packed (4×4) structure of CoP was steadily observed in the potential range between 0 and 0.75 V. When the potential was returned to a value more positive than 0.8 V, the highly ordered (4×4) structure was again changed into a disordered structure as seen in Figure 2.

When the electrode potential was kept more negative than 0 V, the CoP adlayer started to change its structure. Figure 5 shows two STM images, almost at the same location in the area of 50 × 50 nm^2, showing the initial process of the structural change of the CoP adlayer at 0 V. Figure 5a shows an STM image obtained 5 min after the potential was scanned from 0.75 to 0 V, where a monatomic step is seen on the lower left. Compared with the STM image of a CoP adlayer obtained at 0.75 V (Figure 3b), disordered areas of CoP on a terrace are seen to grow in the image obtained at 0 V (Figure 5a). Figure 5b shows an STM image obtained 8 min after the potential scan to 0 V. In this image, CoP molecules are invisible in many areas on the terrace, whereas they are still aligned near the step: the molecules might be slowly desorbing from the terrace and the remaining molecules on the terrace might be mobile. Finally, after 20 min, no molecules were seen on the surface, and reconstructed rows of Au(111) appeared, indicating that CoP molecules were completely desorbed from the surface and that the reconstruction was induced at a cathodic potential.[25] When the electrode potential was set more positive than ca. 1.1 V, the highly ordered arrays became gradually unclear due to the oxidative desorption of CoP (Figure 1b).

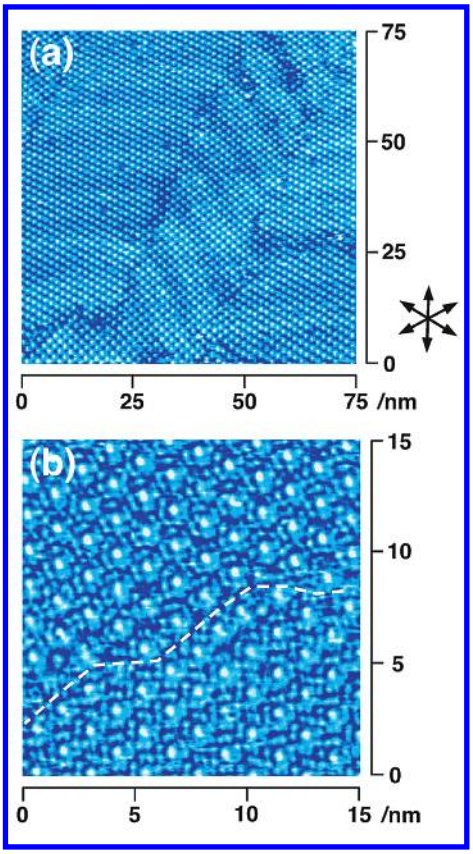

Figure 6. Large-scale (75 × 75 nm^2) (a) and high-resolution (15 × 15 nm^2) (b) STM images of the CoOEP adlayer formed on Au(111) surface in 0.1 M $HClO_4$ acquired at 0.85 V. The potential of the tip was 0.45 V, and tunneling currents were 1.5 nA (a) and 1.25 nA (b). The set of three arrows indicates the close-packed directions of Au(111) substrate.

(2) CoOEP Adlayer. A further investigation was carried out for the adlayer structure of CoOEP on Au(111) to understand the effect of additional ethyl moieties. Figure 6 shows typical STM images of a CoOEP adlayer on Au(111) acquired at 0.85 V in 0.1 M $HClO_4$. Well-ordered domains can be seen on the atomically flat terrace, and individual molecules are recognized even in the large area of 75 × 75 nm^2. Interestingly, long-range modulations are seen as rows on the surface in the STM image, which are separated with a spacing ranging from 6.8 to 9.2 nm on the terrace. The difference in height is only 0.06 nm, which

is much smaller than that of the atomic step. These results show that the transformation of underlying Au atoms from (1×1) to ($\sqrt{3}$×22), or the so-called reconstruction, took place as a result of the adsorption of CoOEP. It is surprising that the reconstruction of the Au(111) surface from (1×1) to ($\sqrt{3}$×22) was induced by the adsorption of CoOEP during immersion in the benzene solution containing CoOEP molecules and that the reconstruction remained even in the aqueous solution at potentials near the OCP. The reason for the reconstruction being induced by the adsorption of CoOEP is not clear, but the following mechanism may be proposed: the adsorbed CoOEP induces a negative charge on the Au(111) surface so that the potential of zero charge of the CoOEP-modified Au(111) shifts to a value more positive than that of bare Au(111) in 0.1 M $HClO_4$.[36] The reconstruction of the Au(111) surface has been shown to be induced also by the adsorption of CoTPP and CuTPP as reported in our recent paper.[25] Figure 6b shows an STM image acquired on an atomically flat terrace in an area of 15 × 15 nm^2, revealing internal molecular structures and orientations in ordered domains. In this image, the domain boundary is also seen, as shown by a white dashed line. Molecular rows in two domains cross each other at an angle of ca. 55°, which suggests that a CoOEP adlayer forms incommensurate structures on the reconstructed Au(111) surface.

To obtain structural details of the CoOEP adlayer, a high-resolution STM image was recorded at 0.85 V. Figure 7a shows a high-resolution STM image acquired in an area of 9 × 9 nm^2, revealing clear internal molecular structures and molecular orientations in the ordered domain. In addition to the information concerning the symmetry and the structure of the CoOEP array, the STM images revealed a great deal of information concerning the internal molecular structure. According to the recent report by Hipps' group, two different molecular orientations of NiOEP exist in UHV.[14] Careful inspection of Figure 7a also allows us to distinguish two different orientations for each CoOEP molecule in molecular rows; i.e., the orientation of each CoOEP molecule in the molecular rows marked by arrows A and B are rotated by ca. 15° from each other. Each CoOEP molecule can be recognized as a square with eight additional spots at the corners corresponding to eight ethyl groups. It is clear that CoOEP molecules possess alternately different orientations in molecular rows marked by arrow A and B. The intermolecular distance along arrows A or B was found to be 1.67 ± 0.07 nm. The intermolecular distance along arrow C was 1.43 ± 0.05 nm. The unit cell of the adlattice is superimposed in Figure 7a. Each unit cell includes two CoOEP molecules, which leads to a surface concentration of 8.7 × 10^{-11} mol cm^{-2}. The details of morphology of each molecule are clearly seen in the height-shaded plot in Figure 7b. The observed features of the image are reminiscent of the molecular structure of CoOEP. A structural model of the CoOEP lattice is shown in Figure 8. The CoOEP adlayer formed an incommensurate structure with respect to the reconstructed Au(111) surface (Figure 6); hence, the exact relation between the CoOEP adlayer and the underlying Au(111) lattice could not be determined.

No potential-dependent structural change was observed in the potential range between 0 and 0.95 V, and the same structure was consistently observed. When the electrode potential was scanned to a value more negative than 0 V, well-ordered arrays gradually became smaller, probably because of a partial desorption of molecules. At electrode potentials more positive than ca. 1.1 V, highly ordered arrays became gradually unclear, and the lifting of reconstruction from ($\sqrt{3}$×22) to (1×1) was observed due to the oxidation of CoOEP (Figure 1c).

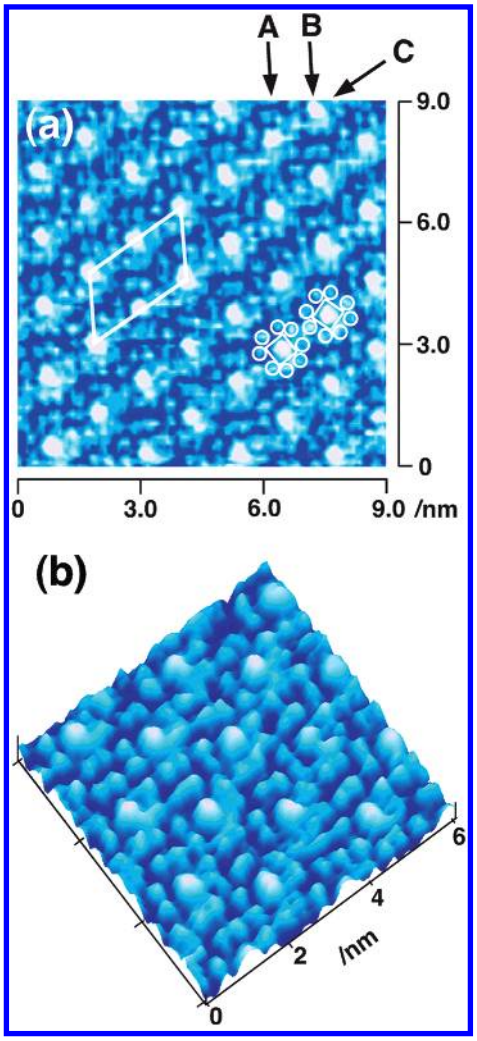

Figure 7. High-resolution (9 × 9 nm^2) STM image (a) and height-shaded plot (b) of the CoOEP adlayer formed on Au(111) in 0.1 M $HClO_4$ acquired at 0.85 V. The potential of the tip and tunneling current were 0.45 V and 0.85 nA, respectively.

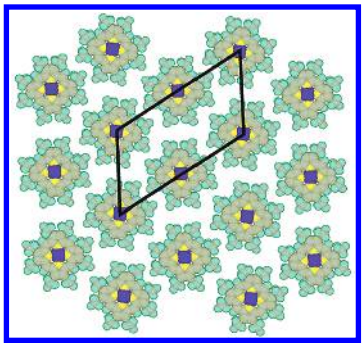

Figure 8. Structural model for CoOEP adlayer on the reconstructed Au(111) surface.

It is of great interest to note that CoOEP molecules induced reconstruction upon adsorption, whereas smaller molecules, CoP, adsorbed in a commensurate manner on Au(111)-(1×1). As can be seen in Figures 6 and 7, CoOEP layers fully cover the Au(111) surface, whereas CoP allows open spaces to remain on Au(111) (Figure 3); for CoOEP, a larger interaction between the molecules and a smaller interaction between the molecules and the surface might be expected compared with the corresponding interactions for CoP. In the case of much larger porphyrins, CoTPP and CuTPP, the adlayers were also densely packed, and the reconstruction from (1×1) to ($\sqrt{3}$×22) took

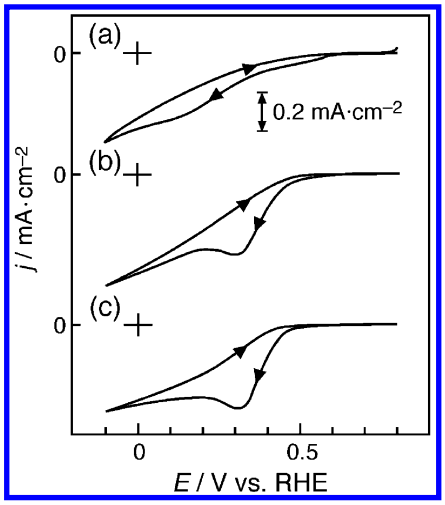

Figure 9. CVs for the O_2 reduction at bare (a), CoP-modified (b), and CoOEP-modified (c) Au(111) electrodes in 0.1 M $HClO_4$ saturated with O_2. The potential scan rate was 50 mV s^{-1}.

place upon adsorption.[25] Further investigations are needed to elucidate the reconstruction of Au(111) upon the adsorption of porphyrins.

Electrocatalytic Activity for O_2 Reduction. On the highly ordered CoP and CoOEP arrays on the Au(111) surface, the reduction of molecular oxygen was examined in 0.1 M $HClO_4$ saturated with O_2. Figure 9 shows the CVs obtained with bare, CoP- and CoOEP-modified Au(111) electrodes. On the bare Au(111) electrode (Figure 9a), a cathodic current due to the reduction of O_2 commenced at ca. 0.55 V, and it increased gradually as the potential was scanned from +0.5 to −0.1 V. On the CoP-modified Au(111) electrode (Figure 9b), the reductive current of O_2 commenced at ca. 0.55 V during the cathodic scan and gave a clear peak for the electrocatalytic reduction of O_2 at 0.32 V. At potentials more negative than 0.3 V, the reductive current still continued to increase gradually. The enhancement of reductive current for O_2 reduction at 0.32 V at the CoP-modified Au(111) electrode compared to that at the bare Au(111) electrode clearly shows that CoP adlayer catalyzes the reduction of O_2. A CoOEP-modified Au(111) electrode also revealed a similarly clear enhancement of the current for the catalytic reduction of O_2 (Figure 9c). At potentials more negative than 0.3 V on the CoOEP-modified electrode, the reductive current remained almost constant because of the process being limited by the diffusion of dissolved O_2. This current limitation by diffusion at potentials more negative than 0.3 V for CoOEP was not observed with CoP, indicating that there is a difference between the electrocatalytic processes on the two different adlayers. As was described in our previous paper, it can be roughly estimated from the current density (ca. 0.4 mA cm^{-2}) that the two-electron reduction of O_2 to H_2O_2 proceeded on the CoTPP-modified Au(111) electrode.[25] Because the reductive current was still observed on the CoP-modified Au(111) at potentials more negative than 0.3 V, the further reduction of H_2O_2 to H_2O might have proceeded partially on the CoP-modified surface.

To analyze the reduction process in further detail, rotating CoP- and CoOEP-modified Au(111) disk electrodes were used. The equation expressing the Koutecky−Levich plot is as follows:

$$1/i_{lim} = 1/i_k + 1/0.62nFD^{2/3}\omega^{1/2}\upsilon^{-1/6}C^* \qquad (1)$$

where i_{lim} is the limiting current. The first term on the right-hand side is the inverse of the kinetic current density, i_k, as expressed by

$$i_k = nFk\Gamma C^* \qquad (2)$$

where n is the number of electrons transferred in the overall electrode reaction, k the rate constant for the catalyzed reaction ($M^{-1}s^{-1}$), Γ the surface concentration of either CoP or CoOEP molecules on the Au(111) surface (mol cm^{-2}), F the Faraday constant, and C^* the concentration of O_2 (mol cm^{-3}). The second term in eq 1 is the inverse of the Levich mass transport limited current density for the reduction of O_2. D, υ, and ω are the diffusion coefficient, the kinematic viscosity of the solution, and the angular rotation speed in rpm, respectively. For the calculation of the slope, the following values were used: υ = 0.01 cm^2 s^{-1},[41] $D = 2.0 \times 10^{-5}$ cm^2 s^{-1},[6] $C^* = 1.2 \times 10^{-3}$ M.[42] Figure 10 shows current−potential curves for the reduction of O_2 at the CoP- and CoOEP-modified Au(111) electrodes. The cathodic scan was started at 0.85 V (near the OCP) for various rotation speeds at the scan rate of 10 mV s^{-1}. The catalytic currents commenced at ca. 0.5 V. The profile observed at the CoP-adsorbed Au(111) electrode was similar to that obtained at the CoTPP-modified Au(111) electrode,[25] suggesting that the reaction is mainly the two-electron reduction of O_2 to H_2O_2. However, the CoP-modified Au(111) gave a slightly larger limiting current density than did the CoOEP. The corresponding Koutecky−Levich plots derived from the limiting

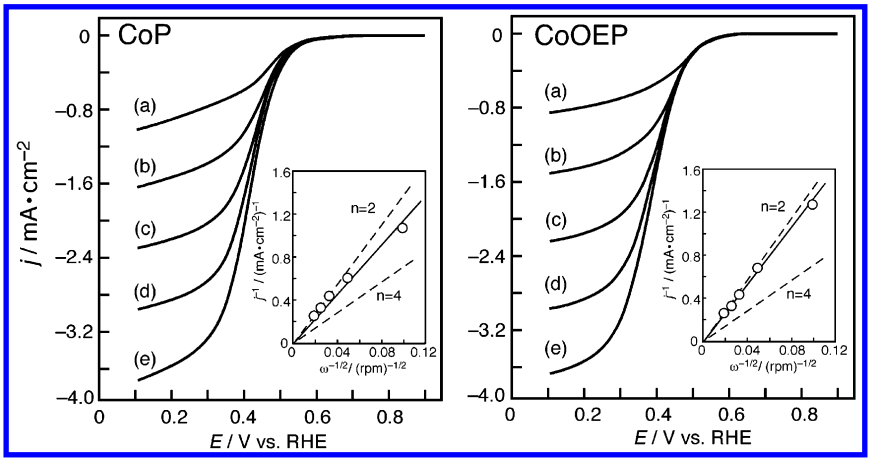

Figure 10. Current−potential curves for the O_2 reduction at rotating CoP-modified (left) and CoOEP-modified (right) Au(111) disk electrodes in 0.1 M $HClO_4$ saturated with O_2. The insets show Koutecky−Levich plots. Rotation speeds were 100 (a), 400 (b), 900 (c), 1600 (d), and 2500 (e) rpm. The potential scan rate was 10 mV s^{-1}.

current density values at 0.1 V in an O_2 saturated solution are shown as the insets in Figure 10. From the slope, the number of electrons, *n*, is calculated to be 2.7 ± 0.1 and 2.1 ± 0.1 for CoP and CoOEP, respectively. These values suggest that, as expected from the CVs in Figure 9 and the current−potential curves in Figure 10 for the reduction of O_2, the 4-electron reduction process of O_2 to H_2O proceeded partially on the CoP-modified Au(111).

It is not clear why the 4-electron process proceeds at CoP. As we discussed in the previous section, interactions between molecules, and between molecule and surface, might affect the electronic state of central Co atom. Or, the distance between the molecules on Au(111) is smaller for CoP (1.18 nm) than for CoOEP (ca. 1.5 nm); thus H_2O_2 produced on CoP molecules in the layer could have further reacted to form H_2O at a neighboring CoP molecule. A systematic investigation is needed to understand more fully the reaction mechanism on porphyrin-modified substrates.

Conclusions

By immersing Au(111) substrate into CoP− and CoOEP−benzene solutions, we succeeded in preparing adlayers of CoP and CoOEP on Au(111) surface and obtaining high-resolution STM images to resolve the packing arrangements and internal molecular structures of adsorbed CoP and CoOEP molecules in aqueous $HClO_4$ solution. CoP molecules formed long-range ordered arrays on Au(111)-(1×1) at applied potentials, whereas CoOEP formed a highly ordered adlayer on the reconstructed Au(111) surface. The O_2 reduction on the CoP-modified Au(111) electrode proceeded mainly via the 2-electron reduction of O_2 to H_2O_2 with a partial participation of the 4-electron reduction to H_2O. On the other hand, the 2-electron reaction was the only reaction path on the adlayer of CoOEP-modified Au(111) electrode.

Acknowledgment. This work was supported in part by Core Research Evolutional Science and Technology organized by Japan Science and Technology Agency (CREST-JST), and by the Ministry of Education, Culture, Sports, Science, and Technology, a Grant-in-Aid for the Center of Excellence (COE) Project, "Giant Molecules and Complex Systems", 2003. We acknowledge Dr. Y. Okinaka for his assistance in writing this manuscript.

References and Notes

(1) *Electron Transfer in Chemistry*; Balzani, V., Ed.; Wiley−VCH: New York, 2001; Vol. 3.
(2) Yeager, E. *Electrochim. Acta* **1984**, *29*, 1527−1537.
(3) Collman, J. P.; Wagenknecht, P. S.; Hutchison, J. E. *Angew. Chem., Int. Ed.* **1994**, *33*, 1537−1554 and references therein.
(4) *Molecular Electronics*; Jortner, J., Ratner, M., Eds.; IUPAC: Oxford, U.K., 1997.
(5) Jasinski, R. *J. Electrochem. Soc.* **1965**, *112*, 526−528.
(6) Guillaud, G.; Simon, J.; Germain, J. P. *Coord. Chem. Rev.* **1998**, *178*−*180*, 1433−1484.
(7) Alt, H.; Binder, H.; Sandstede, G. *J. Catal.* **1973**, *28*, 8−19.
(8) Shi, C.; Steiger, B.; Yuasa, M.; Anson, F. C. *Inorg. Chem.* **1997**, *36*, 4294−4295.
(9) Song, E.; Shi, C.; Anson, F. C. *Langmuir* **1998**, *14*, 4315−4321.
(10) Shi, C.; Anson, F. C. *Inorg. Chem.* **1998**, *37*, 1037−1043.
(11) Jung, T. A.; Schlittler, R. R.; Gimzewski, J. K. *Nature* **1997**, *386*, 696−697.
(12) Yokoyama, T.; Yokoyama, S.; Kamikado, T.; Mashiko, S. *J. Chem. Phys.* **2001**, *115*, 3814−3818.
(13) Yokoyama, T.; Yokoyama, S.; Kamikado, T.; Okuno, Y.; Mashiko, S. *Nature* **2001**, *413*, 619−621.
(14) Scudiero, L.; Barlow, D. E.; Hipps, K. W. *J. Phys. Chem. B* **2002**, *106*, 996−1003.
(15) Scudiero, L.; Barlow, D. E.; Hipps, K. W. *J. Phys. Chem. B* **2000**, *104*, 11899−11905.
(16) Scudiero, L.; Barlow, D. E.; Mazur, U.; Hipps, K. W. *J. Am. Chem. Soc.* **2001**, *123*, 4073−4080.
(17) Itaya, K. *Prog. Surf. Sci.* **1998**, *58*, 121−248.
(18) Kunitake, M.; Batina, N.; Itaya, K. *Langmuir* **1995**, *11*, 2337−2340.
(19) Kunitake, M.; Akiba, U.; Batina, N.; Itaya, K. *Langmuir* **1997**, *13*, 1607−1615.
(20) Ogaki, K.; Batina, N.; Kunitake, M.: Itaya, K. *J. Phys. Chem.* **1996**, *100*, 7185−7190.
(21) Sashikata, K.; Sugata, T.; Sugimasa, M.; Itaya, K. *Langmuir* **1998**, *14*, 2896−2902.
(22) Wan, L.-J.; Shundo, S.; Inukai, J.; Itaya, K. *Langmuir* **2000**, *16*, 2164−2168.
(23) Tao, N. J.; Cardenas, G.; Cunha, F.; Shi, Z. *Langmuir* **1995**, *11*, 4445−4448.
(24) Tao, N. J. *Phys. Rev. Lett.* **1996**, *76*, 4066−4069.
(25) Yoshimoto, S.; Tada, A.; Suto, K.; Narita, R.; Itaya, K. *Langmuir* **2003**, *19*, 672−677.
(26) Neya, S.; Funasaki, N.; *Tetrahedron Lett.* **2002**, *43*, 1057−1058.
(27) Senge, M. O.; Bischoff, I.; Nelson, N. Y.; Smith, K. M.; *J. Porphyrins Phthalocyanines* **1999**, *3*, 99−116.
(28) Adler, A. D.; Longo, F. R.; Kampas, F.; Kim, J. *J. Inorg. Nucl. Chem.* **1970**, *32*, 2443−2445.
(29) Clavilier, J.; Faure, R.; Guinet, G.; Durand, R. *J. Electroanal. Chem.* **1980**, *107*, 205−209.
(30) Honbo, H.; Sugawara, S.; Itaya, K. *Anal. Chem.* **1990**, *62*, 2424−2429.
(31) Yoshimoto, S.; Narita, R.; Itaya, K. *Chem. Lett.* **2002**, 356−357.
(32) Yoshimoto, S.; Narita, R.; Wakisaka, M.; Itaya, K. *J. Electroanal. Chem.* **2002**, *532*, 331−335.
(33) Yoshimoto, S.; Narita, R.; Tsutsumi, E.; Matsumoto, M.; Itaya, K.; Ito, O.; Fujiwara, K.; Murata, Y.; Komatsu, K. *Langmuir* **2002**, *18*, 8518−8522.
(34) Yoshimoto, S.; Tada, A.; Suto, K.; Itaya, K. *J. Phys. Chem. B* **2003**, *107*, 5836−5843.
(35) Abe, T.; Swain, G. M.; Sashikata, K.; Itaya, K. *J. Electroanal. Chem.* **1995**, *382*, 73−83.
(36) Kolb, D. M.; Schneider, J. *Electrochim. Acta* **1986**, *31*, 929−936.
(37) Angerstein-Kozlowska, H.; Conway, B. E.; Hamelin, A.; Stoicoviciu, L. *J. Elctroanal. Chem.* **1987**, *228*, 429−453.
(38) Postlethwaite, T. A.; Hutchison, J. E.; Hathcock, K. W.; Murray, R. W. *Langmuir* **1995**, *11*, 4109−4116.
(39) He, Y.; Ye, T.; Borguet, E. *J. Am. Chem. Soc.* **2002**, *124*, 11964−11970.
(40) *Porphyrins and metalloporphyrins*; Smith, K. M., Ed.; Elsevier/North-Holland Biomedical Press: Amsterdam, 1976.
(41) Zagal, J.; Bindra, P.; Yeager, E. *J. Electrochem. Soc.* **1980**, *127*, 1506−1517.
(42) Markovic, N. M.; Adzic, R. R.; Vesovic, V. B. *J. Electroanal. Chem.* **1984**, *165*, 121−133.